AIAA JOURNAL
Vol. 33, No. 11, November 1995

Model Correlation Using Multiple Static Load and Vibration Tests

D. C. Zimmerman* and T. Simmermacher†
University of Houston, Houston, Texas 77204-4792

In this paper, algorithmic approaches to enhance damage detection and model refinement capability are developed for cases in which experimental data from multiple tests are available. The tests may include both multiple vibration tests and multiple static load tests. The use of multitest measurements are shown to be one method to address a part of the incomplete measurement problem common to system health monitoring and model refinement, namely, the mismatch in the number of measured vibration modes in comparison to the number of modes included in the analytical finite element model. Key points made in the development will be highlighted using numerical experiments.

Introduction

THE need for highly accurate analytical models of flexible structures and machinery is required in order to accurately predict dynamic performance. Owing to the complexity of these structures, a common modeling technique is to use the finite element method. However, it is well known that the "as built" structure rarely matches the dynamic characteristics of the finite element model (FEM). Recent efforts to address this problem have resulted in the development and evaluation of algorithmic methods for structural model refinement. These same algorithms have also demonstrated capability in approaching the system health monitoring problem.

Algorithms used to address FEM refinement can be broadly classified as falling into one of four different approaches, optimal-matrix updates, sensitivity methods, eigenstructure assignment techniques, and minimum-rank perturbation methods. Survey papers providing an overview of these techniques are provided in Refs. 1 and 2.

In the optimal-matrix update formulation, perturbation matrices for the mass, stiffness, and/or damping matrices are determined which minimize a given cost function subject to various constraints. A typical cost function used is the Frobenius norm of the perturbation matrix.[3] Typical constraints may include satisfaction of the eigenproblem for all measured modes, definiteness of the updated property matrices, and preservation of the original sparsity pattern.

Sensitivity methods for model refinement and damage detection make use of sensitivity derivatives of modal parameters with respect to physical design variables[4] or with respect to matrix element variables.[5] When varying physical parameters, the updated model is consistent within the original FE model framework.

Control-based eigenstructure assignment techniques determine the pseudocontrol which would be required to produce the measured modal properties with the initial structural model.[6,7] The pseudocontrol is then translated into matrix adjustments applied to the initial FEM.

Finally, the development of a minimum-rank update theory has been recently proposed as a computationally attractive approach for model refinement and damage detection.[8] The update to each property matrix is of minimum rank and is equal to the number of experimentally measured modes which the modified model is to match.

A problem shared with all developed approaches is that of the incomplete measurement problem. The incomplete measurement problem has two contributions: 1) experimental measurement of a lesser number of modes of vibration than that of the analytical model and 2) experimental measurement of a lesser number of degrees of freedom than that of the analytical model.

One approach to practically address problem 1 is to test the structure under consideration in different configurations and test procedures. Different configurations may include such things as changing boundary conditions and/or altering the mass and stiffness distribution of the structure. Different test procedures may include modal and static loads/displacement testing.

Previous algorithmic approaches for handling multiple configuration test data have mainly been formulated using a sensitivity-based approach. In these approaches, the sensitivity of some objective function and/or eigenvalue problem with respect to physical parameters is utilized to arrive at a set of "optimal" physical parameters.[9–11] In Ref. 9, the approach taken was to minimize the product of the dynamic stiffness and the measured frequency response function (essentially a residual force balance) at a set of discrete frequencies over a range of various testing configurations. In Ref. 10, a sequential linear programming technique was utilized to minimize the required physical parameter changes needed to meet multiple modal test constraint conditions. In Ref. 11, a direct nonlinear optimization approach was used to determine changes to physical parameters using both modal and static test data. The direct approach required repeated finite element analysis to determine the numerical gradients at each step of the optimization.

Notable exceptions to the use of sensitivity-based algorithms are provided in Refs. 12 and 13. In Ref. 12, an approach which utilized a pseudoinverse solution to a multitest orthogonality condition was shown to provide a minimum-norm adjustment to the stiffness matrix. Finally, the multiboundary condition testing approach advanced in Ref. 13 updates selected terms in the mass and stiffness matrix using a least-squares approach. The experimental data utilized in the approach is obtained from multiple tests in which testing support constraints, or boundary conditions, are moved.

In this work, we extend the theory of minimum rank perturbation theory[8] (MRPT) for the case where both different configurations and different test type data (modal and static) are available. Rather than dealing with physical parameters, the minimum-rank perturbation theory determines a symmetric stiffness perturbation matrix that improves the correlation of measured and analytical test data.

Stiffness Modification Using Measured Modal/Static Test Data

Prior development of MRPT has focused on the case where experimental data are available from a single modal test. Following a brief review, the results presented in this section extend MRPT to the case where experimental data are available from multiple modal and static tests.

Received March 15, 1994; revision received Jan. 4, 1995; accepted for publication Jan. 5, 1995.

*Associate Professor, Department of Mechanical Engineering. Member AIAA.

†Graduate Student, Department of Mechanical Engineering. Student Member AIAA.

Single Modal Test Data

In this section, a brief overview of minimum-rank perturbation theory for undamped structures is presented in which the mass matrix is assumed correct. In addition, the experimental eigenvectors and analytical model are assumed to be of equal dimension. This is true 1) when all FEM degrees of freedom (DOF) are measured, 2) after the application of an eigenvector expansion algorithm,[14,15] or 3) after the application of a FEM reduction algorithm.[16,17] The problem to be solved is to determine a minimum-rank perturbation to the stiffness matrix such that the measured and analytical modal properties are in agreement. The eigenvalue problem for the structure can be written as

$$\left(\lambda_{di}^2 M + K\right)v_{di} = \Delta K_d v_{di} \equiv \boldsymbol{d}_i \qquad i = 1, \ldots, p \tag{1}$$

where it is assumed that p eigenvalues and eigenvectors have been measured. In Eq. (1), M and K are the $n \times n$ mass and stiffness matrices, the matrix ΔK_d represents the stiffness modeling error to be determined, v_{di} is the ith measured eigenvector, and λ_{di} is the corresponding eigenvalue. Equation (1) can be written in matrix form as

$$\begin{gathered} MV_d\Lambda_d + KV_d = \Delta K_d V_d \equiv B \\ \Lambda_d = \operatorname{diag}\left(\lambda_{d1}^2, \lambda_{d2}^2, \ldots, \lambda_{dp}^2\right) \\ V_d = [v_{d1}, v_{d2}, \ldots, v_{dp}] \\ B = [\boldsymbol{d}_1, \boldsymbol{d}_2, \ldots, \boldsymbol{d}_p] \end{gathered} \tag{2}$$

It should be noted that B can be calculated from Eq. (2) in terms of the original FEM matrices and the measured modal properties. The matrix B also summarizes the mismatch between the analytical model and the measured modal properties (the dynamic residual). The solution of Eq. (2) for ΔK_d is given by

$$\Delta K_d = B\left(B^T V_d\right)^{-1} B^T \tag{3}$$

A detailed mathematical derivation investigating the properties associated with this solution is provided in Ref. 8. The dimension of the matrix to be inverted in Eq. (3) is equal to the number of measured modes used in the update. At this point, the refined stiffness matrix $(K - \Delta K_d)$ does not maintain the sparsity pattern (load paths) of the original stiffness matrix. For situations where sparsity preservation is an important requirement, an iterative alternating projections technique has been developed.[15]

Multiple Modal Test Data

An inherent limitation of the MRPT update is that the rank of the update is less than or equal to the number of measured modes. The case that the rank is less than the number of measured modes implies that the number of measured modes exceeds the number required to perform an accurate update. This limitation is actually a strength when approaching the damage detection problem, as most localized forms of damage manifest themselves as small rank changes to the stiffness and/or mass matrices. However, for the model correlation problem, modeling errors can be both local and global in nature. Global modeling errors typically will result in larger rank changes. Thus, for the model correlation problem an obvious question is: Were enough modes measured?

In performing a modal test, there typically exists an upper frequency above which there is no attempt to measure modes of vibration. This is due to 1) the use of a finite number of sensors, 2) inability to excite the structure above a certain frequency, and 3) corruption of global modes by local modes of vibration. One practical way to provide additional modal information about the structure is to perform a series of modal tests in which the mass and/or stiffness distribution of the structure has been altered in each test. Assuming that q such tests have been performed, Eq. (2) can be written as

$$\Delta K_d[V_{d1} \mid V_{d2}|\cdots|V_{dq}] \equiv \Delta K_d \hat{V}_d = [B_1 \mid B_2|\cdots|B_q] \equiv \hat{B} \tag{4}$$

where V_{dj} are the measured eigenvectors of the jth test and B_j is the dynamic residual associated with the jth test:

$$B_j = [M + \Delta M_j]V_{dj}\Lambda_{dj} + [K + \Delta K_j]V_{dj} \tag{5}$$

In Eq. (5), ΔM_j and ΔK_j are the mass and stiffness perturbations made to the baseline structure for the jth modal test. The perturbation matrix ΔK_d is easily calculated as

$$\Delta K_d = \hat{B}\left(\hat{B}^T \hat{V}_d\right)^{-1} \hat{B}^T \tag{6}$$

Note that this formulation utilizes all measured data simultaneously to arrive at the stiffness perturbation matrix. There is no constraint that the same number of measured modes be obtained in each separate test.

Multiple Static Test Data

In this section it is assumed that static load data are available in the form of measured forces and resulting deflections. With these assumptions, the static test data can be represented as

$$\begin{aligned} &K[\boldsymbol{x}_1|\cdots|\boldsymbol{x}_r] + [\Delta K_1\boldsymbol{x}_1|\cdots|\Delta K_r\boldsymbol{x}_r] - [\boldsymbol{f}_1|\cdots|\boldsymbol{f}_r] \\ &\quad = \Delta K_d[\boldsymbol{x}_1|\cdots|\boldsymbol{x}_r] \equiv \Delta K_d X_s = B_s \end{aligned} \tag{7}$$

where $\{\boldsymbol{x}_j, \boldsymbol{f}_j\}$ represent one of this r static deflection/load pairs and ΔK_j, $j = 1, r$, represents any change in the stiffness distribution from the nominal configuration to the jth test. The matrix B_s represents the static residual. Again, Eq. (7) can be solved for ΔK_d as

$$\Delta K_d = B_s\left(B_s^T X_s\right)^{-1} B_s^T \tag{8}$$

Multiple Modal and Static Test Data

From the prior developments it is trivial to show that the MRPT can also be used to determine ΔK_d when both static and modal data are available. Essentially, Eq. (4) can be augmented with static data X_s and B_s:

$$\begin{aligned} &\Delta K_d[V_{d1} \mid V_{d2}|\cdots|V_{dq} \mid X_s] \\ &\quad \equiv \Delta K_d \bar{V}_d = [B_1 \mid B_2|\cdots|B_q \mid B_s] \equiv \bar{B} \end{aligned} \tag{9}$$

with solution

$$\Delta K_d = \bar{B}\left(\bar{B}^T \bar{V}_d\right)^{-1} \bar{B}^T \tag{10}$$

Symmetry Considerations

In the calculation of ΔK_d using Eqs. (3), (6), (8), or (10), the symmetry of ΔK_d requires the matrix which is inverted be symmetric.[8] In the case of perfect, noise-free measurements, it can easily be shown that this condition is met. In the case of noisy measurements, the requirement for Eq. (3) to yield a symmetric solution is for the measured eigenvectors to be mass orthogonal. Thus, techniques to optimally orthogonalize measured modes[3] can be used to modify the measured eigenvectors such that when used in Eq. (3) yield a symmetric ΔK_d. Simple computational techniques to modify the measured data to enforce symmetry in the remaining three cases are not apparent.

The inability to modify the measured data to ensure a symmetric perturbation matrix is, in fact, not a major reason for concern. Experience gained in comparing exact, noise corrupted, and optimally orthogonalized eigenvectors in various numerical studies indicates that the orthogonalized vectors are closer to the true eigenvectors roughly half of the time in comparison to the noise-corrupted vectors. In other words, the effect of orthogonalization is not to necessarily reduce the distance between the measured eigenvector and the true eigenvector.

An equally valid way to generate a symmetric perturbation matrix is to utilize the fact that in the MRPT formulation there is no contribution of the true eigenvector to the nonsymmetric portion of the calculated ΔK_d. Viewed in another way, the degree of nonsymmetry in the calculated perturbation matrix is an indirect measure of the noise contained in the measurements. The calculated perturbation ΔK_d can be written as

$$\Delta K_d = \Delta K_{d_{\text{true}}} + \Delta K_{d_{\text{noise}_{\text{sym}}}} + \Delta K_{d_{\text{noise}_{\text{nsym}}}} \tag{11}$$

where $\Delta K_{d_{\text{true}}}$ is the symmetric perturbation matrix that would be calculated if all measurements were exact, $\Delta K_{d_{\text{noise}_{\text{sym}}}}$ is a symmetric perturbation matrix calculated due to the portion of the noise that yields a symmetric matrix, and $\Delta K_{d_{\text{noise}_{\text{nsym}}}}$ is the nonsymmetric perturbation matrix due to the portion of the noise that yields a nonsymmetric matrix. In a certain sense, the optimal orthogonalization procedure drives $\Delta K_{d_{\text{noise}_{\text{nsym}}}}$ to zero but may decrease or increase $\Delta K_{d_{\text{noise}_{\text{sym}}}}$. Thus, it is justifiable to retain the symmetric portion of the calculated perturbation matrix $[(\Delta K_d + \Delta K_d^T)/2]$ as the matrix used for model correlation. This argument holds true for the case of multiple modal test data augmented with static load data.

Selection of Residual Vectors

In Eqs. (2), (4), (7), and (9), a decision must be made on whether to use all possible residual vectors, where we now refer to a column of any of the B matrices as a residual vector. The choice is governed by two factors: 1) the rank of the true modeling error perturbation matrix (which is actually unknown) and 2) the linear independence of the residual vectors, eigenvectors, and static deflections.

The rank of the true modeling error perturbation matrix can be estimated in a number of ways. In the no measurement noise case, the residual vectors will have only nonzero elements at DOFs that have been mismodeled. Using finite element connectivity information, one can determine which elements have been mismodeled. Summing the rank of each mismodeled elemental matrix yields the rank of the true modeling error perturbation matrix. Of course, noise destroys the perfect zero/nonzero pattern of the residual, so this technique only provides an estimate of the true rank.

Another technique to estimate the rank is to calculate the singular values of the residual matrix B. If the matrix is of full rank, then the rank of B provides a lower limit to the true rank of the modeling error perturbation matrix. The residual matrix can be rank deficient for two reasons: 1) either the rank of the true modeling error is less than the column dimension of the residual matrix or 2) the lower limit of the true rank is equal to the column dimension of the residual matrix but the residual vectors are linearly dependent due to insignificant differences in the various testing configurations. To see a simple example of when the latter situation arises, consider a hypothetical problem in which a modal test is performed on the nominal structure, as well as a single mass loaded structure. Although theoretically the residual vectors from the two different testing configurations will be linearly independent, they will become numerically dependent as the mass loading tends to zero. In other words, the additional residual vectors generated from the second test do not provided numerically significant new information. Two numerical techniques have been investigated to reduce the column dimension of the residual matrix such that the resulting matrix is well conditioned.

Subset Selection

The problem of subset selection has been studied extensively in the context of the rank-deficient least-squares problem (min $\|A\boldsymbol{x}-\boldsymbol{b}\|_2$) when the rank deficiency is due to redundancy among the factors which comprise the underlying model. The problem studied is to determined which parameters (elements of $\boldsymbol{x}$), and their associated columns of A, best capture the observed data and the underlying model.[18] A heuristic solution procedure has been developed which utilizes the singular value decomposition (SVD) of A and application of the QR algorithm with column pivoting to the right singular vectors.

In our application, we can view the residual matrix B as A and determine which columns contain independent information. The heuristic column selection procedure outlined in Ref. 18 does not depend on the observation vector $\boldsymbol{b}$, which for our application does not exist. Given the residual matrix $B \in \mathcal{R}^{n\times p}$ (n = number of FEM DOFs, p = total number of residual vectors), the Chan[19] SVD for the singular values and right singular vectors, followed by a QR decomposition of a submatrix of the right singular vector requires approximately $np^2 + (17/3)p^3 + n\hat{p}^2 - (1/3)\hat{p}^3$ flops, where $\hat{p}$ is an estimate of the rank of the full residual matrix. It is important to note that the flop count varies linearly with FEM dimension. The reduced dynamic residual contains $\hat{p}$ columns of B. The stiffness perturbation matrix constraint equations are then written using only the $\hat{p}$ columns of B and the corresponding columns of V.

Subspace Selection

For all types of data, the MRPT perturbation matrix constraint equation is given in generalized form by Eq. (9). The subspace selection algorithm is defined to be the search for a matrix $Z \in \mathcal{R}^{p\times\hat{p}}$ such that

$$\Delta K_d \bar{V}_d Z = \bar{B} Z \tag{12}$$

is well conditioned. The unknowns at this point are $\hat{p}$, the numerical rank of $\bar{B}$, and Z. Consider the singular value decomposition of $\bar{B}$ defined as

$$\bar{B} = \left[\overset{\hat{p}}{U_1} \mid U_2\right] \begin{bmatrix} \Sigma & 0 \\ 0 & 0 \end{bmatrix} [V_1 \mid V_2]^T \tag{13}$$

where $\Sigma \in \mathcal{R}^{\hat{p}\times\hat{p}}$ is the matrix of nonzero singular values (or singular values greater than some prescribed tolerance) and the left and right singular vectors U and V are partitioned conformable. When $\bar{B}$ is rank deficient, the range of $\bar{B}$ is spanned by the $\hat{p}$ columns of U_1. Thus, it is desired to find a Z such that

$$\bar{B} Z = U_1 \tag{14}$$

The matrix Z can be approximated by utilizing the pseudoinverse of $\bar{B}$ as

$$Z = \bar{B}^+ U_1 = V_1 \Sigma^+ U_1^T U_1 = V_1 \Sigma^+ \tag{15}$$

Note that the left singular vector $\boldsymbol{U}_1$ does not have to be explicitly formed and saved. The calculation of Z using the Chan[19] SVD is $np^2 + (17/3)p^3$ flops. It is important to note that the flop count varies linearly with FEM dimension. The solution of Eq. (12) is then given by

$$\Delta K_d = \bar{B} Z \left(Z^T \bar{B}^T \bar{V}_d Z\right)^{-1} Z^T \bar{B}^T \tag{16}$$

Unlike the subset selection technique, which constrains the reduced constraint equation to consist of columns of the full constraint equation, the subspace selection technique attempts to extract out the maximum information from all residual vectors. It is apparent that the subspace selection algorithm can also be used to reduce the effects of measurement noise for the case that the number of residual vectors exceeds the rank of the true stiffness perturbation matrix.

Examples

In this section several examples are presented that highlight key points made throughout the paper. For the first two examples, the "numerical test bed" consists of a beam model of a structure similar to the NASA HMB-2R test structure.[20] A stick figure of the two-dimensional beam model is shown in Fig. 1. With 41 3-DOF nodes, the model has a total of 123 DOFs. Because static data are required to evaluate the techniques, it is assumed that testing takes place with node 1 cantilevered. It should be noted that the development of this model was motivated by studies on substructure modeling and model refinement presented in Ref. 21.

Preservation of Symmetry

In this example, the two techniques previously discussed for preserving symmetry in the updated model are compared. The first technique, which is valid for only single modal test data, is to mass orthogonalize the measured eigenvectors. The second technique, which essentially just ignores the nonsymmetric portion of the calculated perturbation matrix, is valid for multiple test configurations/data. In particular, consider the case in which there is a 90% reduction in stiffness of the beam connecting nodes 5–6 of the model and the first ten modes of vibration have been "measured." As

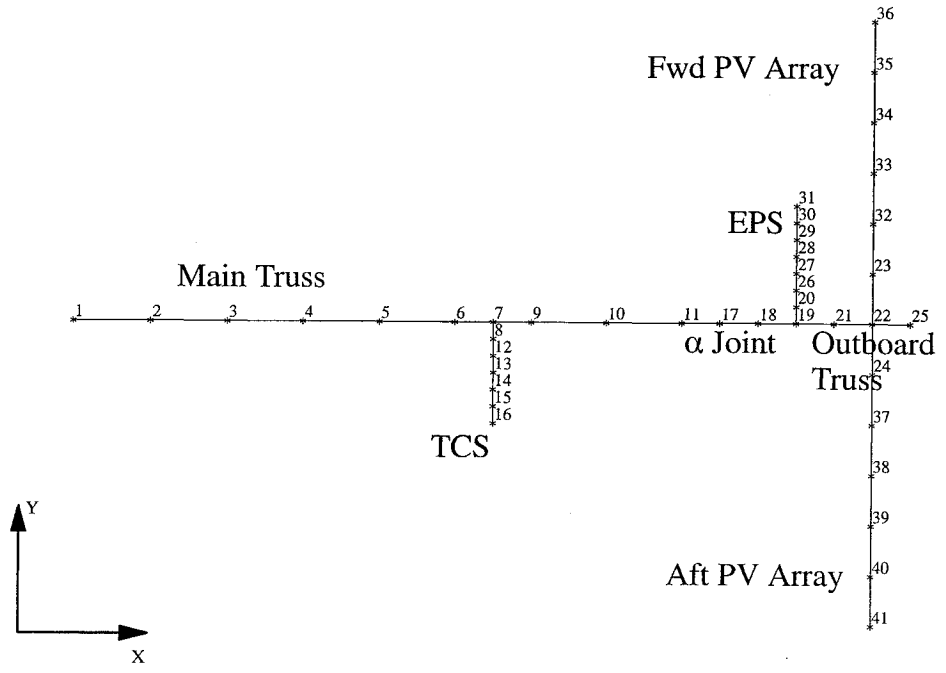

Fig. 1 Stick figure of model.

a measure of how well the damage is estimated and the differences between the two techniques, consider the performances measures

$$E_1 = \left(\|\Delta K_{d_{\text{true}}} - \Delta K_{d_{\text{est}}}\|_f\right) / \left(\|\Delta K_{d_{\text{true}}}\|_f\right) \quad (17a)$$

$$E_2 = \left(\|\Delta K_{d_{\text{ignore}}} - \Delta K_{d_{\text{orth}}}\|_f\right) / \left(\|\Delta K_{d_{\text{true}}}\|_f\right) \quad (17b)$$

where $\Delta K_{d_{\text{true}}}$ is the actual stiffness change due to damage, $\Delta K_{d_{\text{est}}}$ is the estimate of damage provided by one of the two methods, $\Delta K_{d_{\text{ignore}}}$ is the estimate of damage when the nonsymmetric portion of the calculation is ignored, $\Delta K_{d_{\text{orth}}}$ is the estimate of damage when the measured modes are mass orthogonalized, and $\|\cdot\|_f$ is the Frobenius norm. Essentially, E_1 compares how well either technique approximates the true damage, whereas E_2 compares the two estimates directly.

Using noise-free modes 8–10, the measure E_1 was evaluated to be $5e^{-13}$, indicating that noise-free modes 8–10 provide rich enough information to accurately estimate the damage. To simulate the case of noisy measurements, the eigenvectors were corrupted with random noise of the form

$$\hat{\phi}_{ij} = \phi_{ij} + \phi_{ij}(\alpha/100)\,\text{rand}(-1, 1) + \text{rms}(\phi_{\cdot j})(\beta/100)\,\text{rand}(-1, 1) \quad (18)$$

where ϕ_{ij} is the ith component of the jth mode, α and β are scale and bias noise factors, respectively, rms(−) is the root mean square operator, rand $(-1, 1)$ is a random number uniformly distributed between -1 and 1, and $\hat{\phi}_{ij}$ is the noise-corrupted eigenvector element. As was shown in Ref. 22, the introduction of the bias noise factor greatly influences the model refinement performance.

Figure 2 shows the performance measures for the case where $\beta = 0.1$ and α is varied between 1 and 19 in increments of 2. For each level of noise, 25 different random cases were run with the plotted values of E_1 and E_2 representing the average over all cases. The upper plot is of E_1, where the solid line corresponds to the case where the nonsymmetric portion of the perturbation is ignored and the circles correspond to the case where the eigenvectors are mass orthogonalized. It is obvious that there is little difference between the two approaches. To see this more clearly, the lower plot is of E_2. The differences between the two approaches is well within the numerical accuracy of the software implementation.

Selection of Residual Vectors: No Noise

In this problem, the beam elements connecting nodes 7–9, 19–21, and 27–28 have been mismodeled. Thus, the true rank of the stiffness mismodeling error is nine. It is assumed that two modal tests have

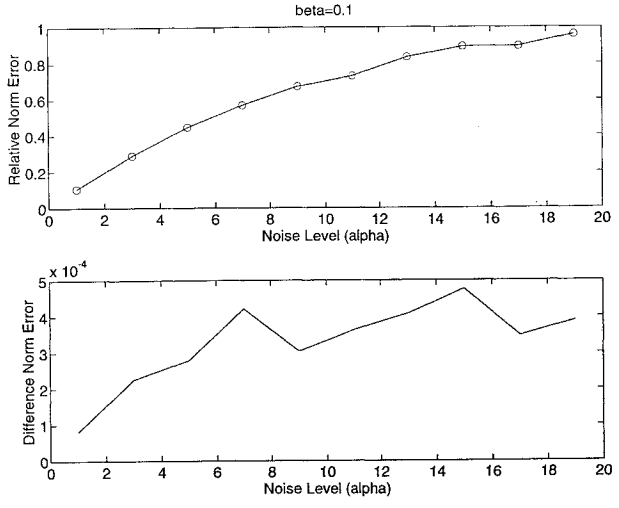

Fig. 2 Comparison of symmetry approaches.

been performed, as well as five static load tests. In the modal tests, the first six modes of vibration are assumed to be measured. The first modal test utilizes the nominal structure as shown in Fig. 1. The second modal test places a discrete mass at node 31, the tip of the electrical power system (EPS). This was done to induce greater modal participation of the EPS in the lower modes of vibration. The static tests placed unit loads at nodes $25y$, $-36x$, $-41x$, $31x$, and $16x$. For simplicity, the modes from the first test will define residual vectors 1–6, the modes from the second test will define residual vectors 7–12, and the remaining static vectors will define residual vectors 13–17.

Figure 3 shows the performance results of selecting three, six and nine residual vectors using the subset selection algorithm. The upper left figure is a plot of the diagonal elements of stiffness modeling error matrix ($\Delta K_{d\,\text{true}}$). Notice that the modeling errors vary greatly in magnitude; in fact, the stiffness modeling error of element 27–28 is barely visible (around DOF 75). The remaining three plots provide a measure of the percent relative error between the diagonal of the true modeling error vs the estimated modeling error defined as

$$E_{3i} = 100\left(\Delta K_{d_{\text{true}}ii} - \Delta K_{d_{\text{est}}ii}\right)/(X_{ii})$$

$$X_{ii} = \Delta K_{d_{\text{true}}ii} \quad \text{if DOF } i \text{ is mismodeled}$$

$$X_{ii} = K_{ii} \quad \text{if DOF } i \text{ is modeled correctly} \quad (19)$$

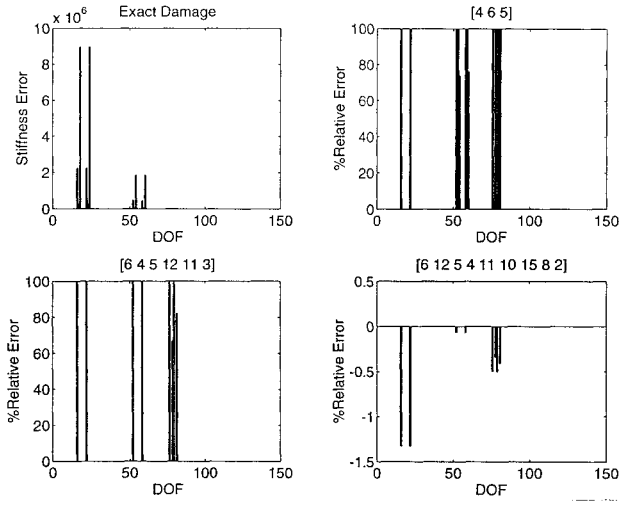

Fig. 3 Subset selection algorithm performance.

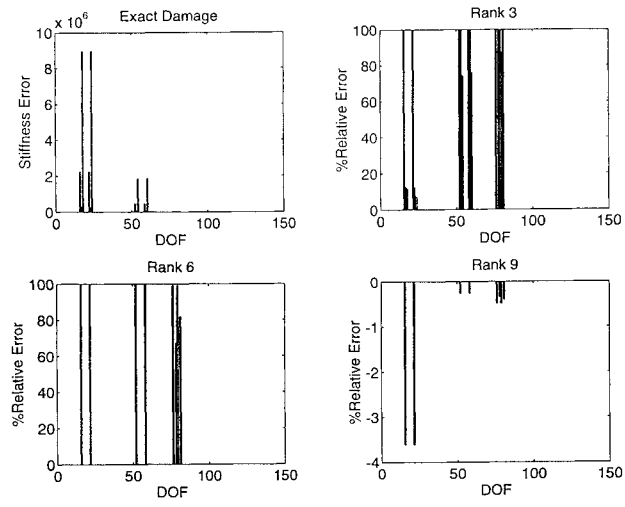

Fig. 4 Subspace selection algorithm performance.

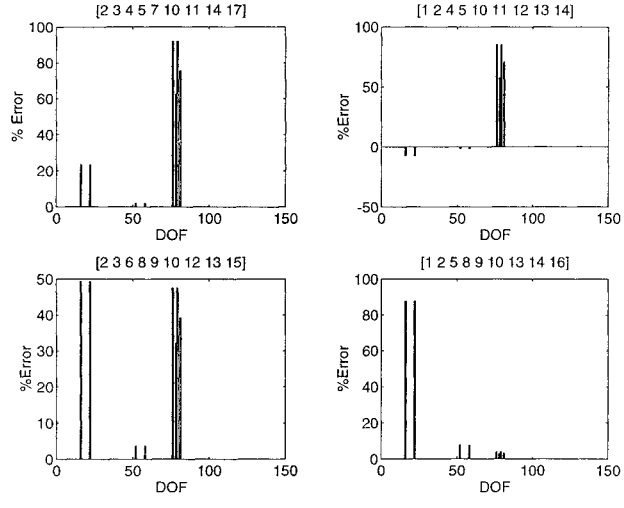

Fig. 5 Random selection performance.

For a DOF that is mismodeled, Eq. (19) provides a relative measure as to how close the estimated modeling error is to the truth. For a DOF that is not mismodeled, Eq. (19) provides a relative measure as to the extent that the model has been inappropriately changed. The numbers over each plot indicate which modes have been used in the extent calculation.

For the case that only three residual modes are used, the subset selection algorithm chooses the highest three modes of the first modal test. The higher modes of vibration typically are chosen in that their more complex deflection pattern increases the chance that a given mode has reasonable strain energy in all three mismodeled elements. For nodes 7–9, the modeling error in the y and Θ_z directions have been significantly reduced; there still is approximately 100% error in the x direction. Note that x motion for this element is axial. For nodes 19–21, the modeling error in the Θ_z direction has been reduced to around 70%; there is still approximately 100% error in the x and y directions. For nodes 27–28, the error in all directions is still approximately 100%.

For the case that six residual vectors are used, the subset selection algorithm chooses the highest four modes of the first modal test and the highest two modes from the second modal test. Errors essentially remain at nodes 7–9 and 19–21 in the x direction, and at nodes 27–28 in the x and Θ_z directions.

Finally, when the algorithm uses nine residual vectors, which is equal to the rank of the true modeling error, the algorithm is able to capture the true modeling error to within less than 1.5% maximum relative error. In theory, the algorithm should calculate the exact modeling error at this point. However, because the measured mode shapes and static vectors have 1) low levels of axial motion of the main and outboard truss sections and 2) low levels of transverse bending of the EPS section, there is numerical precision errors remaining at 1) nodes 7–9 and 19–21 in the x direction and 2) nodes 27–28 in the x and Θ_z directions.

The results of using the subspace selection algorithm for this problem is summarized in Fig. 4. The same trends as observed for the subset selection algorithm are seen when using the subspace selection algorithm. The labels above each plot corresponds to the estimate of $\hat{p}$ used in the update procedure.

To demonstrate the importance of using a meaningful selection algorithm, Fig. 5 presents the performance of the update algorithm for four different cases in which nine residual vectors are chosen at random. The labels above each plot correspond to the residual vectors used in the calculation. Note that the performance of the update algorithm is severely degraded when residual vectors are chosen at random even in the case of noise-free measurements.

Selection of Residual Vectors: With Noise

In this problem, the effect of measurement noise on the performance of the selection algorithm and update algorithm is considered. Instead of using the earlier model, a smaller uniform cantilever beam model is used. The reasons for changing to this model are twofold. First, the HMB-2R motivated beam model is constructed of components whose effective bending stiffness differ by orders of magnitude. This has been shown in many model refinement algorithms to cause a highly nonuniform effect of noise on the update result, making a meaningful comparison of the two selection algorithms difficult. Second, working with a smaller model allows for a clearer graphical presentation of the results.

Consider a cantilever beam modeled with 10 equal length beam elements. A 20-DOF FEM is used to model the healthy structure. Experimental data of the damaged structure are created by solving the eigenproblem for a FEM model in which Young's moduli of the third and seventh element from the cantilever end are both reduced by 50%. It is assumed that the first 10 modes of vibration are measured. The eigenvectors are corrupted with noise as defined by Eq. (18).

In Fig. 6, the upper left plot shows a three-dimensional view of the true mismodeling error. The large peaks corresponds to those degrees of freedom which have been mismodeled. Peaks associated with rotational DOFs are not visible as their modeling errors are two orders of magnitude smaller than the translational components. The upper right plot is the residual vector calculated using the noise-free fundamental mode. In each grouping, the large peaks correspond to translational DOFs, whereas the smaller peaks correspond to rotation.

Both selection algorithms require an estimate of the rank of the true modeling error matrix and/or the rank of the residual matrix. Three different rank estimation measures using the singular values σ have been presented in Ref. 23. The first measure sets a rank tolerance of $\hat{p}$, where $\sigma(\hat{p}+1)/\sigma(1)$ is less than some specified tolerance. The second measure specifies a rank tolerance of $\hat{p}$ for

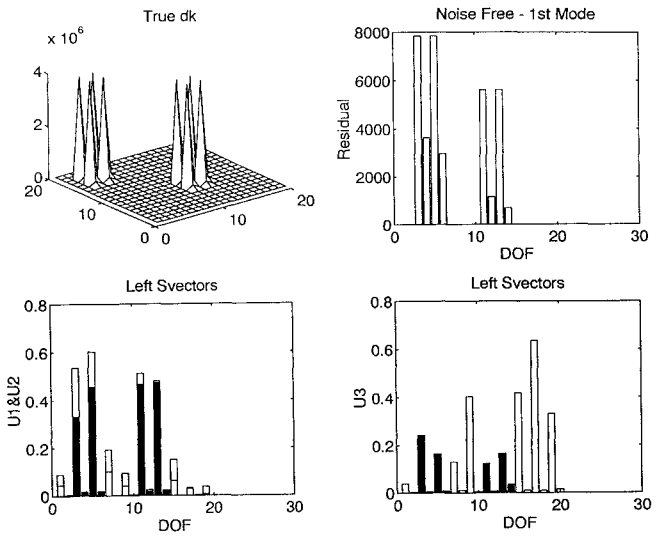

Fig. 6 Modeling error and residuals.

which $\sigma(\hat{p})/\sigma(\hat{p}+1)$ is largest. The third measure is based on the cumulative percent of variance and is a measure of the percentage of "information" that is represented by the first $\hat{p}$ singular values. The value of $\hat{p}$ is selected at the point at which the cumulative percent of variance falls above a preselected value. By definition, the first and third measures require a user-defined limit, whereas the second measure is based purely on the singular values. In this example, the first tolerance was set to $1e^{-4}$ (four orders of magnitude rolloff), and the third measure tolerance was set at 90%. The estimated rank $\hat{p}$ was taken to be the minimum over all three measures.

For the case that the noise factors are selected as $[\alpha\ \beta] = [20\ 3]$, $\hat{p}$ is estimated to be two. The true rank of the modeling error is four. The lower left plot in Fig. 6 is the first two column vectors of $\bar{B}Z$ as defined in Eq. (14). The lower right plot is of the third column vector of $\bar{B}Z$. The darkened bars are associated with DOFs which have been mismodeled. In the lower left plot, the darkened bar height corresponds to the minimum component of the two vectors. From the lower left plot one can see that the subspace selection algorithm residual vectors have large peaks at the mismodeled translational DOFs. However, the noise has caused peaks to appear at other translational DOFs which are significantly higher than the peaks at the mismodeled rotational DOFs. In post-analysis, the lower right plot confirms the rank estimate; the next most significant column of $\bar{B}Z$ (the third) contains no consistent information. This is true for all remaining columns of $\bar{B}Z$.

Figure 7 shows the calculated stiffness perturbation matrix for the case that the noise parameter α is varied and $\beta = 3.0$. The values of noise parameters $[\alpha\ \beta]$ and the selection technique (subspace or subset) are indicated in the heading. Thus, each row has the same noise added to the eigenvectors, and each column uses the same selection algorithm. In all noise cases, $\hat{p}$ was estimated to be two. In the subset selection algorithm, the two best modes were always calculated to be modes nine and ten. In comparing the left and right columns of Fig. 7, it is seen that the subspace selection algorithm is able to better approximate the true modeling error in comparison to the subset selection algorithm.

Finally, Fig. 8 shows the performance of the update algorithm when no selection algorithm is used and the rank of the update is estimated using the residual vectors in conjunction with finite element model connectivity. The upper left bar plot shows all 10 residual vectors. An analysis of the residual vectors would indicate that two elements are damaged, each of which is modeled by a rank two finite element. Therefore, the rank of the update is selected to be four. The estimate is correct; however, this approach for selecting the rank of the update has no knowledge that the noisy data does not contain rich enough information to support a rank four update. The remaining plots show the calculated update for the noise case [20 3], where the selected modes are also shown in brackets. In the brackets, $[a : b]$ implies that modes a through b were used. The upper right plot utilizes the four best modes as

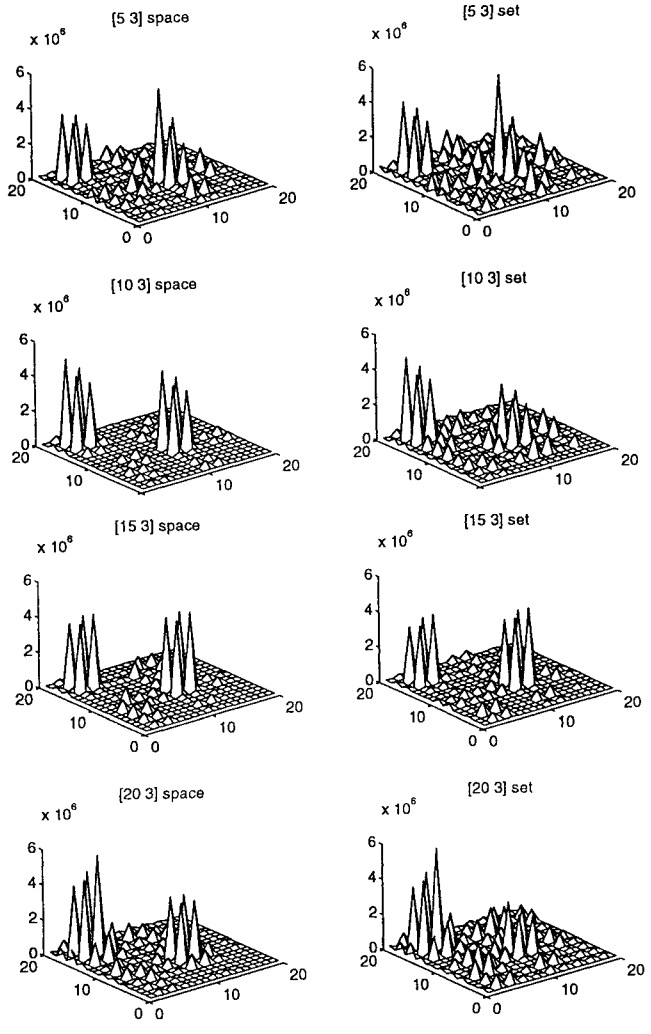

Fig. 7 Effect of noise on subspace/subset selection.

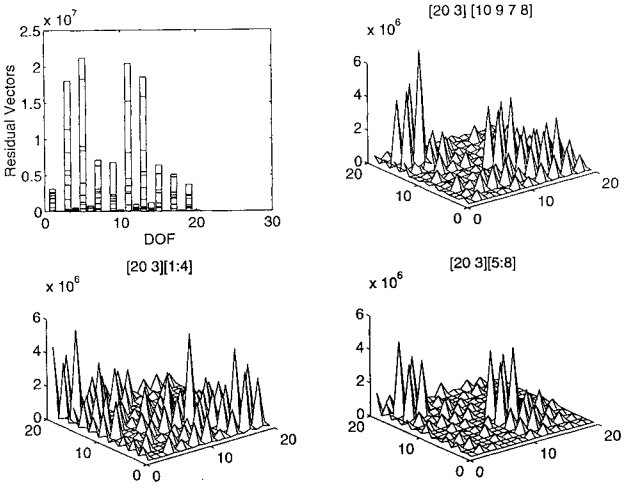

Fig. 8 Effect of ignoring rank of residual matrix.

determined by the subset selection algorithm. The other two sets of modes were picked heuristically. The importance of properly choosing the rank of the update consistent with the information contained in the residual matrix, as well as the use of a mode selection algorithm, is evident in comparing the update results in Fig. 8 to those of Fig. 7.

Summary

In conclusion, the minimum rank perturbation theory based model refinement and health monitoring approach has been extended to

the case in which experimental data are available from a suite of experiments. The experiments may be either modal surveys or static load/displacement tests. In any given test, the structure may be perturbed from the nominal condition by the addition/subtraction of mass and/or stiffness.

Numerical studies have indicated that often the eigenvectors and/or static displacements from one test are nearly linear combinations of the eigenvectors and static displacements from other tests, resulting in an ill-conditioned residual matrix. To address this issue, two residual vector selection algorithms were developed. One approach is based on the subset selection process typically encountered in solving rank-deficient least-squares problem. The second approach involves an abstraction of the minimum rank perturbation theory in that residual vectors calculated from eigenvectors and static displacements are replaced by generalized residual vectors. As a side note, this study demonstrates the importance of pretest planning, in that a given test is only worth effort if it provides substantially new information.

References

[1]Ibrahim, S. R., and Saafan, A. A., "Correlation of Analysis and Test in Modeling of Structures, Assessment and Review," *Proceedings of the 5th International Modal Analysis Conference*, Union College, Schenectady, NY, 1987, pp. 1651–1660.

[2]Heylen, W., and Sas, P., "Review of Model Optimization Techniques," *Proceedings of the 5th International Modal Analysis Conference*, Union College, Schenectady, NY, 1987, pp. 1177–1182.

[3]Baruch, M., and Bar Itzhack, I. Y., "Optimum Weighted Orthogonalization of Measured Modes," *AIAA Journal*, Vol. 16, No. 4, 1978, pp. 346–351.

[4]Martinez, D., Red-House, J., and Allen, J., "System Identification Methods for Dynamic Structural Models of Electronic Packages," *Proceedings of the AIAA/ASME/ASCE/AHS/ASC 32nd Structures, Structural Dynamics, and Materials Conference* (Baltimore, MD), AIAA, Washington, DC, 1991, pp. 2336–2346.

[5]Matzen, V. C., "Time Domain Identification of Reduced Parameter Models," *Proceedings of the Society for Experimental Mechanics Spring Conference on Experimental Mechanics* (Houston, TX), Society for Experimental Mechanics, Inc., Bethel, CT, 1987, pp. 401–408.

[6]Zimmerman, D. C., and Widengren, W., "Model Correction Using a Symmetric Eigenstructure Assignment Technique," *AIAA Journal*, Vol. 28, No. 9, 1990, pp. 1670–1676.

[7]Inman, D. J., and Minas, C., "Matching Analytical Models with Experimental Modal Data in Mechanical Systems," *Control and Dynamics Systems*, Vol. 37, Academic, 1990, pp. 327–363.

[8]Zimmerman, D. C., and Kaouk, M., "Structural Damage Detection Using a Minimum Rank Update Theory," *Journal of Vibration and Acoustics*, Vol. 116, No. 2, 1992, pp. 222–231.

[9]Lammens, S., Heylen, W., Sas, P., and Brown, D., "Model Updating and Perturbed Boundary Condition Testing," *Proceedings of the 11th International Modal Analysis Conference* (Kissimmee, FL), Union College, Schenectady, NY, 1993, pp. 449–455.

[10]Chen, K., Brown, D., and Nicolas, V. T., "Perturbed Boundary Condition Model Updating," *Proceedings of the 11th International Modal Analysis Conference* (Kissimmee, FL), Union College, Schenectady, NY, 1993, pp. 661–667.

[11]Hajela, P., and Soeiro, F. J., "Structural Damage Detection Based on Static and Modal Analysis," *Proceedings of the AIAA/ASME/ASCE/AHS/ASC 30th Structures, Structural Dynamics, and Materials Conference* (Mobile, AL), AIAA, Washington, DC, 1989, pp. 1172–1181.

[12]Berman, A., and Fuh, J.-S., "Structural System Identification Using Multiple Tests," *Proceedings of the AIAA Dynamic Specialist Conference* (Long Beach, CA), AIAA, Washington, DC, 1990, pp. 99–104.

[13]Wada, B. K., Kuo, C. P., and Glaser, R. J., "Extension of Ground-Based Testing for Large Space Structures," *Proceedings of the AIAA/ASME/ASCE/AHS/ASC 26th Structures, Structural Dynamics, and Materials Conference* (Orlando, FL), AIAA, Washington, DC, 1985, pp. 477-483.

[14]Berman, A., and Nagy, E. J., "Improvements of a Large Analytical Model Using Test Data," *AIAA Journal*, Vol. 21, No. 8, 1983, pp. 1168–1173.

[15]Zimmerman, D. C. and Kaouk, M., "Eigenstructure Assignment Approach for Structural Damage Detection," *AIAA Journal*, Vol. 30, No. 7, 1992, pp. 1848–1855.

[16]Guyan, R. J., "Reduction of Stiffness and Mass Matrices," *AIAA Journal*, Vol. 3, No. 2, 1965, p. 380.

[17]McGowan, P. E., "Dynamic Test/Analysis Correlation Using Reduce Analytical Models," M.S. Thesis, Engineering Mechanics, Old Dominion Univ. Norfolk, VA, Aug. 1991.

[18]Golub, G. H., and VanLoan, C. F., *Matrix Computations*, Johns Hopkins Univ. Press, Baltimore, MD, 1983, pp. 162–179.

[19]Chan, T. F., "An Improved Algorithm for Computing the Singular Value Decomposition," *Association for Computing Software Transaction on Mathematical Software*, Vol. 8, 1982, pp. 72–83.

[20]McGowan, P. E., Edighoffer, H. E., and Wallace, J. W., "Development of an Experimental Space Station Model for Structural Dynamics Research," NASA TM-102601, 1990.

[21]Widrick, T. W., "Determining the Effect of Modal Truncation and Modal Errors in Component Mode Synthesis Methods," M.S. Thesis, George Washington Univ. Joint Inst. for the Advancement of Flight Science, Hampton, VA, July 1992.

[22]Kim, H. M., and Bartkowicz, T., "Damage Detection and Health Monitoring of Large Space Structures," *Proceedings of the AIAA/ASME/ASCE/AHS/ASC 34th Structures, Structural Dynamics, and Materials Conference* (La Jolla, CA), AIAA, Washington, DC, 1983, pp. 3527–3533.

[23]Juang, J.-N., and Pappa, R. S., "An Eigensystem Realization Algorithm for Modal Parameter Identification and Model Reduction," *Journal of Guidance, Control, and Dynamics*, Vol. 8, No. 5, pp. 620–627.